Research Article

Dharmender Singh Rana, Nagesh Thakur, Sourbh Thakur, and Dilbag Singh*

Electrochemical determination of hydrazine by using MoS_2 nanostructure modified gold electrode

https://doi.org/10.37819/nanofab.007.190
Received Nov 24, 2021; accepted Dec 30, 2021

Abstract: In this paper, MoS_2 nanostructure was synthesized by using ammonium molybdate and thiourea as precursors through annealing in a tube furnace. The nanostructure was characterized for morphological, structural and elemental composition by using a field emission scanning electron microscope (FESEM), powder X-ray diffraction and energy-dispersive X-ray spectroscopy (EDS). The as-synthesized nanostructure was then immobilized on the gold electrode (working electrode) for the electrochemical detection of hydrazine. Cyclic voltammogram shows an intense peak at 22 μA, which proved the high electrocatalytic ability of the sensor. The strong electrocatalytic activity regarding the oxidation of hydrazine is ascribed to good electron transfer ability and high surface area of the nanoparticles. Further, the chronoamperometric study was conducted to estimate the sensitivity and the detection limit of the sensor. The sensor exhibited a detection limit and sensitivity of 196 nM and 5.71 μA/μM cm^2 respectively. Promising results such as high electrical conductivity, lower detection limit and high sensitivity of the as-synthesized MoS_2 nanostructure have proved its potential towards the electrochemical detection of hydrazine.

Keywords: MoS_2 nanostructure, Hydrazine sensing, Cyclic voltammetry, Amperometry

1 Introduction

Rapid industrial growth and the overpopulation of developing countries have posed a great threat to sustainable development. In the last decade, environmental pollution has increased many folds which substantially divert the focus of current research towards remediation of environmental pollution. Among these, water pollution has adversely affected the ecosystem and human health. Therefore, it is our prime focus to address water pollution to fulfill the clean water requirement worldwide [1]. After scrutinizing the major water polluting sources, it has been found that industrial waste, which is discarded directly into the aquatic system has created havoc [2]. These waste contaminants such as chemical and pesticides are generally stable and highly soluble in water as a result persist in the environment for a longer time and hence pollute the freshwater [3].

Among different water pollutants, hydrazine is one of the major contributors. It finds application in a wide range of sectors such as catalysis [4], emulsifier [5], high-power rocket propellant [6], reagent in industrial and agriculture sector [7], corrosion inhibitor in boilers [8], fuel cells [9] and a starting material in the production of different herbicides, insecticides [10], pesticides [11] and pharmaceutical compounds. Furthermore, it is also utilized as a precursor in the production of colorants and foaming agents [12]. It is classified under Group 2B carcinogen by the United States Environmental Protection Agency [13]. Adverse health impacts associated with exposure to a high quantity of hydrazine are nausea, headache, seizures, dizziness, irritation in the respiratory tract, abnormalities in blood and dysfunctioning of the central nervous system, brain and liver [14, 15]. Its wide applicability in different fields in spite of its ill effects causes a threat to the living organism. Therefore, to avoid the health impacts of hydrazine it is the need of the hour to sense it below its permissible limits. Different techniques, which have already been reported in the literature regarding the sensing of hydrazine are flow injection with chemiluminescent detection [16], gas chromatography [17], high-performance liquid chromatography (HPLC) [18], absorption and emission spectrophotometry [19, 20]. These methods require a long time for analysis, sophisti-

***Corresponding Author: Dilbag Singh:** Department of Environmental Sciences, Central University of Himachal Pradesh, Dharamshala, Kangra (H.P.) India; Email: dilbagrana@hpcu.ac.in
Dharmender Singh Rana: Department of Physics, Himachal Pradesh University, Summer Hill, Shimla (H.P.) India; Department of Physics, MLSM College Sunder Nagar, Mandi (H.P.) India
Nagesh Thakur: Department of Physics, Himachal Pradesh University, Summer Hill, Shimla (H.P.) India
Sourbh Thakur: Department of Organic Chemistry, Bioorganic Chemistry and Biotechnology, Silesian University of Technology, B. Krzywoustego, Poland

cated instrumentation and complicated process regarding the preparation of the sample. Therefore, the electrochemical methods with advantageous properties such as accuracy, simplicity, cost-effectiveness and high sensitivity, are considered as the best alternative to these methods [21]. The mechanism associated with the electrochemical detection of hydrazine includes its oxidation on the electrode's surface. Generally, a modified working electrode is preferable over a bare electrode due to the slow kinetics associated with the latter. The key requirement regarding the modification of the working electrode is relatively low overpotential for the oxidation of hydrazine and high current response [22, 23]. Although, noble metal-based materials such as gold [24], silver [25] and platinum [26] show high conductivity the high cost and scarcity limit their applications. Different 2D materials such as hexagonal boron nitride (h-BN) [27, 28], black phosphorous (BP) [29], bismuthine [30], antimonene [31], borophene [32], mxene [33], graphene [34, 35], transition metal carbides [36], transition metal oxide [37], pyridyl-based organochalcogen [38] have emerged as most promising after the discovery of graphene due to their wide applicability in the area of material science, condensed matter physics and engineering [39, 40]. However, different limitations such as zero or low bandgap of graphene, BP and large bandgap of h-BN limit their use in the electronics applications. On the other side, transition metal dichalcogenides (TMDs), a new class of 2D materials with significant potential in different fields such as optoelectronics, electronics [41] and energy storage applications [42] has gained tremendous attention. These are atomically thin semiconductors of MX_2 type where M represents the transition metals such as molybdenum and tungsten and X refers to the sulfur atoms. These nanomaterials possess high structural stability owning to the covalent bond between the sulfur layer and the transition metals. Moreover, different layers of these materials are stacked through weak Van der Waals forces and the distance that exists between the molybdenum sheets is 0.65 nm [43]. Weak Van der Waals forces allow easy exfoliation of these materials through mechanical and chemical means. Generally, a bulk form of these material shows the properties of silicon-like semiconductors and possess an indirect bandgap (1.23 eV), while the direct bandgap of 1.89 eV is displayed by the monolayers of TMDs. The direct bandgap of TMD sheets is due to the confinement of electrons in the single plane [44]. Moreover, MoS_2 exhibits the tunable bandgap and different methods for adjusting its bandgap are chemical modification [45], applying compressive strain [46] and implication of vertical electrical field [47]. These materials also play an efficient role in chemical and biosensing. Due to these properties of MoS_2, it has become the focus of researchers for electrochemical applications. Moreover, literature has also proven the superiority of nanomaterials of TMDs over bulk MoS_2 regarding electrochemical performance.

Inspiring from the above facts, we have employed MoS_2 nanostructure for the electrochemical detection of hydrazine. The nanostructure was prepared through the thermal annealing method in a tube furnace. The flat 2D material is employed for the modification of gold electrodes, where it is proved to be an excellent electron mediator for the electrochemical oxidation of hydrazine. This work paves a way to design new 2D materials which provide more active sites on the edge and surface.

2 Materials and Method

2.1 Chemicals required

Ammonium molybdate tetrahydrate, (<99% purity) was taken from Sigma Aldrich. Thiourea (<97% purity), bought from CDH, was used as a source of sulfur. Hydrazine was supplied by Sigma Aldrich and used as received. A stock solution of hydrazine (1.0 mM) in 0.1 M phosphate buffer solution was prepared before being used in the experiment and the waste was discarded after the completion of the experiment. Deionized water used in the experiment was prepared in a double distillation unit.

2.2 Synthetic procedure of MoS_2 nanostructure

The MoS_2 nanostructure was prepared through the thermal annealing method using ammonium molybdate tetrahydrate and thiourea as starting materials. In brief, 200 mg of ammonium molybdate tetrahydrate and 1.0 g of thiourea were dissolved in 50 ml of distilled water separately. Then thiourea solution was mixed with ammonium molybdate under constant stirring. The solution mixture was then sonicated for thirty minutes and dried in the oven at 50°C after stirring on a magnetic stirrer. The resultant mixture was heated at 500°C for five hours under a nitrogen atmosphere leads to the formation of black colored fine powder.

2.3 Characterization

To investigate the morphology of the MoS_2 nanoparticles, field emission scanning electron microscopy (FESEM) was employed. FESEM images were recorded by using FESEM JEOL JSM-7610F (Tokyo, JAPAN). Further, the energy disper-

sive spectroscopy (EDS) was employed to investigate the elemental and chemical compositions of the as-prepared nanomaterials by using OXFORD EDS, attached with FE-SEM. The crystallinity and crystal phases were studied by an X-ray diffractometer (XRD) (D8 Discover, Bruker AXS, Karlsruhe, Germany). The XRD spectra were measured with Cu-Kα radiation (k = 1.54056 Å) at 45 kV and 40 mA in the range of 2θ = 10–80° with a scan speed of 8°/min. The electrochemical characterization of the nanomaterial was performed at Autolab Type-III cyclic voltammeter.

2.4 Electrode preparation for the electrochemical sensing of hydrazine

In the first step, the gold electrode (working electrode) was polished with alumina slurry and activated through the ultrasonication method in a mixed solution of deionized water and ethanol. The electrode was then washed thoroughly to remove a trace amount of alumina. Then the electrode was left to dry in an oven at 60°C. In the second step, the MoS_2 nanostructure was immobilized onto the surface of the gold electrode (Au electrode). Before fabrication of the electrode, a slurry of the nanostructure of MoS_2 was prepared by adding butyl carbitol acetate (BCA). A 5.0 µL of the prepared slurry was then cast over the gold electrode, followed by dropping the solution of Nafion. After that, the modified Au electrode was subjected to a temperature of 60°C under a nitrogen atmosphere. The electrochemical study was preceded by Autolab Type-III cyclic voltammeter. Three electrodes-based systems was there in cyclic voltammeter where, in addition to the working electrode, counter (Pt wire) and reference electrodes (Ag/AgCl (sat. KCl) were also present. A 0.1 M Phosphate buffer solution (pH = 7) was also used in the experiment. Additionally, amperometric studies were performed to study the effect of the concentration of hydrazine on the current.

3 Results and Discussion

3.1 Characterizations of MoS_2 nanostructure

FESEM technique was employed for analysing the surface features of the as-synthesized MoS_2 nanostructure and the images are shown in Figure 1. Figure 1(a) and 1(b) represents the typical low and high magnification FESEM, which confirm the formation of flat sheet type nanostructure.

Additionally, crumpled and flaky nanostructure over the nanosheet of MoS_2 was also observed, where different

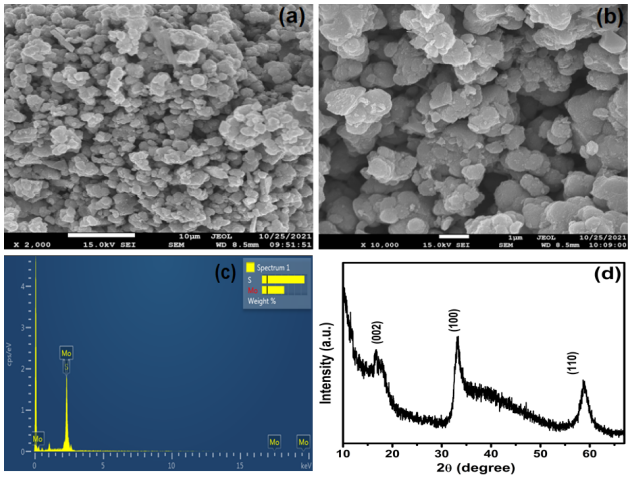

Figure 1: Typical (a) low and (b) high-magnification images of FESEM, (c) EDS spectra and (d) XRD pattern of as-synthesized MoS_2 nanostructure

sized flakes are overlapped over each other in a random fashion giving a graphitic appearance. The average length of the nanosheet was 0.65 µm. The EDS coupled with FE-SEM was employed for examining the elemental composition of the MoS_2 nanostructure. The EDS spectra of the as-synthesized nanostructure is shown in Figure 1(c). Well-defined peaks in the EDS spectra were referred to as the molybdenum (Mo) and sulfur (S) atoms. Further, any other peak corresponding to other impurity elements was not found in the EDS spectra, which confirms the formation of pure MoS_2.

The crystallinity and crystal phase associated with the as-synthesized MoS_2 nanostructure was analysed by using XRD studies. Figure 1(d) displays the XRD pattern of the MoS_2 nanostructure. Series of well-defined diffraction reflections at 2θ values 16.6, 33.2 and 58.8° are found corresponding to (002), (100) and (110) planes. The reflection plane (002) corresponds to a d-spacing of about 0.62 nm and the peak broadening suggested that the material is layered nanostructure. A Slight shift to the lower angle side has also been observed in comparison to JCPDS card 01-075-1539 for hexagonal molybdenum sulfide, which indicates a slight widening of the basal plane [48].

3.2 Detection of hydrazine by using MoS_2 modified Au electrode

Electrocatalytic activity of the as-synthesized MoS_2 nanocomposite towards hydrazine was assessed by cyclic voltammetry (CV). The experiment was run in 0.1 M phosphate buffer solution (PBS) at pH = 7. Figure 2 displayed

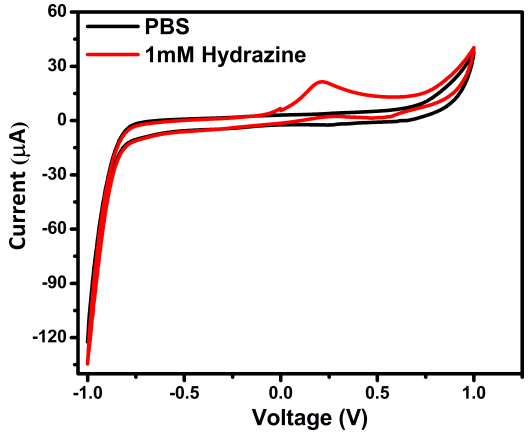

Figure 2: CV curve of MoS_2 modified Au electrode in 0.1 M PBS with and without 1.0 mM hydrazine at the 100 mV/s scan rate

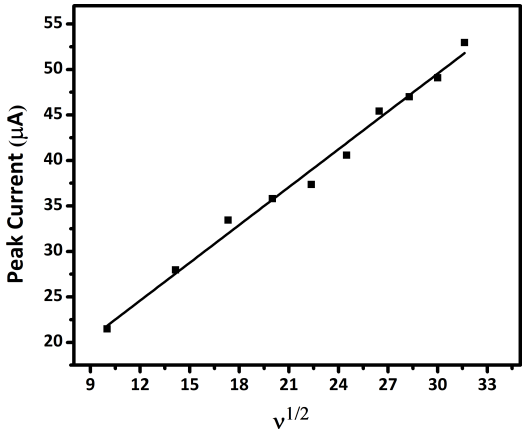

Figure 4: A plot of MoS_2 modified Au electrode, representing the relationship between the anodic peak current and the square root of scan rate ($\nu^{1/2}$)

the CV response of the Au electrode after its modification with MoS_2 in the absence (black line) and the presence (red line) of 1 mM hydrazine at a scan rate of 100 mV/sec. Modified Au electrode did not give any peak in the absence of hydrazine, while a sharp current peak has been observed after the addition of hydrazine. The sensor displayed the anodic peak (22 μA) of hydrazine at a potential of 0.27 V. The absence of cathodic peak shows the irreversible nature, which is due to the excellent electrocatalytic effect regarding the detection of hydrazine. Hydrazine donates electrons to MoS_2 nanoparticles and increases the conductivity of the latter, hence improving the electrocatalytic activity by facilitating the charge transfer kinetics. Hydrazine, as a reducing agent, is increasing the intra-particle conductivity of the MoS_2 nanoparticles. Based on the above results, it can be concluded that MoS_2 nanomaterial is suitable for electrocatalytic and sensing applications.

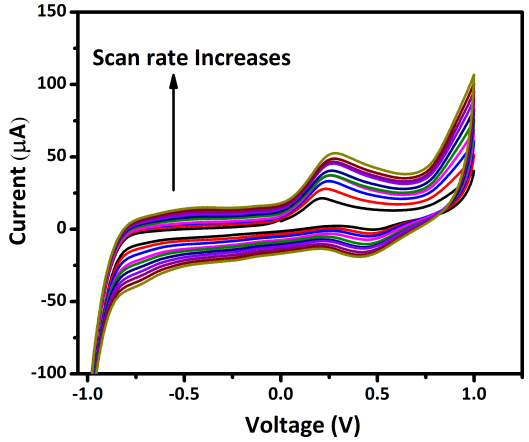

Figure 3: CV curves of MoS_2 modified Au electrode for 1.0 mM hydrazine in 0.1 M PBS at 100 to 1000 mV/s scan rate with a successive increment of 100 mV/s

Electrochemical properties of the MoS_2 modified Au electrode have been further investigated by observing its current response at different potential sweeps ranging from 100 to 1000 mV/sec with a successive increment of 100 mV/s (Figure 3). It was inferred from the peak that the anodic current peak increased in a linear pattern (Figure 4) with the increased scan rate. Additionally, a slight shift in peak potential toward the positive side has also been observed. The positive intercept of Figure 4 distinctly reveals that the process of oxidation is diffusion-controlled and ruled out any possibility of adsorption of hydrazine molecules on the electrode surface [49].

Further, the number of electrons that participated in the hydrazine's oxidation was estimated through the Randles-Sevcik equation [50]

$$I_p = \left(2.99 \times 10^5\right) n^{3/2} A\, D^{1/2} \nu^{1/2} C$$

where I_p = peak current, A = surface area of the electrode (cm^2), n = sum of electrons that participated in redox cycle, ν = potential of scan rate (V/s), D = diffusion coefficient (cm^2/s) and C = the amount of N_2H_4 in bulk solution (mol cm^{-3}). On the basis of the above equation, the number of electrons estimated to participate in the reaction was two and the suggested chemical reaction was [50]

$$H_2N - NH_2 + \frac{5}{2}OH^- \longrightarrow \frac{1}{2}N_3^- + \frac{1}{2}NH_3 + \frac{5}{2}H_2O + 2e^-$$

The main purpose of this study is to explore the reliability or the efficiency of the MoS_2 as a sensor for the detection of hydrazine. Chronoamperometry study was performed to record the current response of MoS_2 modified gold electrode with the change in hydrazine concentration at a constant potential of 0.27 V. The transient in current with the alteration in the concentration (0.1 to 1.0 μM) of hydrazine

Table 1: Comparative study of different nanomaterials utilized for the sensing of hydrazine

S. No.	Nanomaterial	Linear detection range	Detection limit	Reference
1.	CuO nanomaterial	0.025–1.66 mM	1.2×10^{-5} M	[52]
2.	hZnS@Au nanoparticles	2 μM–24.22 mM	0.667 μM	[53]
3.	Poly(dopamine)	100 μM–10 mM	1 μM	[54]
4.	Cobalt(II) phthalocyanine	20–200 μM	0.5 μM	[55]
5.	Co_3O_4 nanowire	20–700 μM	0.5 μM	[56]
6.	Pd-modified TiO_2 electrode	1–20 mM	0.023 mM	[57]
7.	MoS_2 nanoparticles	0.1–1 μM	0.196 μM	This work

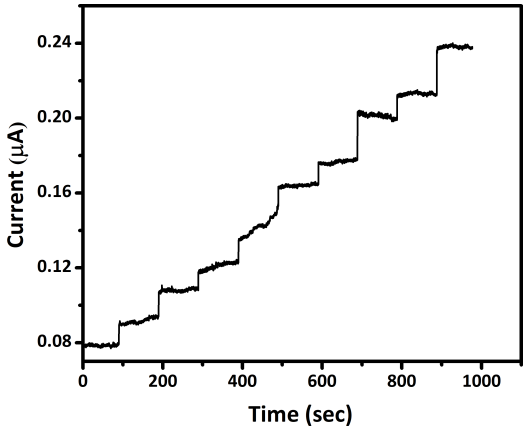

Figure 5: The amperometric response of the MoS_2 modified Au electrode after the consecutive addition of N_2H_4 (0.1 to 1 μM) into 0.1 M PBS at pH 7.0 with a time interval of 100 s

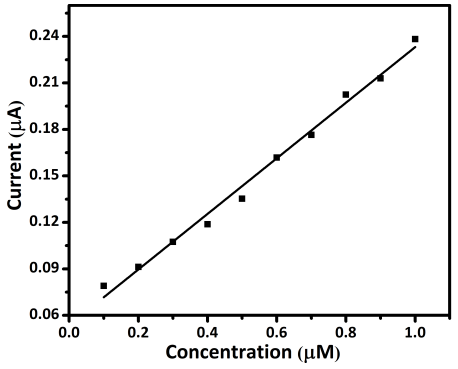

Figure 6: The variation of peak current versus concertation of MoS_2 modified gold electrode in amperometric titrations

was recorded (Figure 5). The current response of the hydrazine displayed a linear response with the increasing amount of hydrazine. Further, different analytical properties such as limit of detection and sensitivity were calculated from the calibration curve (Figure 5).

The detection limit found for MoS_2 regarding the detection of hydrazine was 196 nM. The value of correlation coefficient (R) calculated was 0.991 for the MoS_2 modified Au electrode. A sensitivity of 5.71 μA/μM cm^2 for MoS_2 was obtained after applying the equation i.e., *the slope of calibration curve/area of the electrode* [51].

Further, the detection limit of as-synthesized MoS_2 nanostructure was compared with the already reported sensors. Table 1 depicts the comparison of different nanomaterials used for the sensing of hydrazine in terms of the limit of detection.

3.3 Selectivity study of MoS_2 nanostructure

Further, as synthesized MoS_2 nanostructure was tested for the interference of various other potential ions (Na^+, Ca^{2+}, K^+, NO^{3-}, SO_4^{2-}) and electro-active species (glucose and urea), through chronoamperometric studies. In this study, the current response of these species (concentration 10-fold) was recorded at the same condition. No interference of these competing ions and electro-active species was recorded. Therefore, it can be concluded that MoS_2 based sensors displayed high selectivity toward the detection of hydrazine.

4 Conclusion

This study represents the sensing of hydrazine through MoS_2 nanostructure. The MoS_2 nanostructure is synthesized through the thermal annealing method. The presence of sulfur atoms in the MoS_2 nanoparticles acts as a catalyst for the oxidation of hydrazine on its surface due to its electron-donating ability. MoS_2 modified gold electrode exhibited an excellent electrocatalytic response toward the sensing of hydrazine with the low limit of detection (196 nM) and high sensitivity (5.71 μA/μM cm^2). Based on the above result, it can be concluded that MoS_2 nanoparticles have a high electrocatalytic ability and can be utilized as a sensor for sensing environmental pollutants.

Conflict of interest: There are no conflicts to declare.

Author contributions: DS is involved at every stage of compilation starting from identifying the problem, compilation of manuscript and internal revision. DSR has collected and compiled all the literature, drawn the figures and written the manuscript under the supervision of DS and NG. ST has assisted the internal revision of the manuscript.

Ethical approval: The conducted research is not related to either human or animal use.

References

[1] Yao L, Yang H, Chen Z, Qiu M, Hu B, Wang X. Bismuth oxychloride-based materials for the removal of organic pollutants in wastewater. Chemosphere. 2021;273:128576. https://doi.org/10.1016/j.chemosphere.2020.128576

[2] Li MF, Liu YG, Zeng GM, Liu N, Liu SB. Graphene and graphene-based nanocomposites used for antibiotics removal in water treatment: a review. Chemosphere. 2019;226:360–380. https://doi.org/10.1016/j.chemosphere.2019.03.117

[3] Kaur N, Khunger A, Wallen S, Kaushik A, Chaudhary GR, Varma RS. Advanced green analytical chemistry for environmental pesticide detection. Current Opinion in Green and Sustainable Chemistry. 2021:100488. https://doi.org/10.1016/j.cogsc.2021.100488

[4] Shimizu W, Nakamura S, Sato T, Murakami Y. Creation of high-refractive-index amorphous titanium oxide thin films from low-fractal-dimension polymeric precursors synthesized by a sol–gel technique with a hydrazine monohydrochloride catalyst. Langmuir. 2012;28(33):12245-12255. https://doi.org/10.1021/la3015139

[5] Deng Q, Slaný M, Zhang H, Gu X, Li Y, Du W, et al. Synthesis of alkyl aliphatic hydrazine and application in crude oil as flow improvers. Energies. 2021;14(15):4703. https://doi.org/10.3390/en14154703

[6] Troyan JE. Properties, production, and uses of hydrazine. Ind. Eng. Chem. 1953;45(12):2608-2612. https://doi.org/10.1021/ie50528a020

[7] Mäeorg U, Ragnarsson U. Synthesis, application and scope of a new protected hydrazine reagent. Tetrahedron Letters. 1998;39(7):681-684. https://doi.org/10.1016/S0040-4039(97)10634-7

[8] Fontana MG. CORROSION Hydrazine for corrosion inhibition. Ind. Eng. Chem. 1955;47(10):81A-82A. https://doi.org/10.1021/ie50550a010

[9] Yamada K, Yasuda K, Fujiwara N, Siroma Z, Tanaka H, Miyazaki Y, et al. Potential application of anion-exchange membrane for hydrazine fuel cell electrolyte. Electrochemistry Communications. 2003;5(10):892-896. https://doi.org/10.1016/j.elecom.2003.08.015

[10] Xing JH, Xia XJ, Peng WL, Fu QM, Chen J, Yu LJ, et al. Synthesis and bioactivity of novel insecticide ZJ0967 [J]. Chinese Journal of Pesticide Science. 2008:2. https://en.cnki.com.cn/Article_en/CJFDTotal-NYXB200802027.htm

[11] Cardulla F. Hydrazine. Journal of Chemical Education. 1983;60(6):505. https://doi.org/10.1021/ed060p505

[12] Byrkit GD, Michalek GA. Hydrazine in organic chemistry. Ind. Eng. Chem. 1950;42(9):1862-1875. https://doi.org/10.1021/ie50489a046

[13] Integrated Risk Information System (IRIS). Hydrazine/Hydrazine Sulfate (CASRN 302-01-2), U.S.E.P.A. (EPA). 2021. https://iris.epa.gov/static/pdfs/0352_summary.pdf

[14] Kirk RE, Othmer DF, Grayson M, Eckroth D. Kirk-Othmer Concise Encyclopedia of chemical technology. Wiley. 1985. https://www.semanticscholar.org/paper/Kirk-Othmer-Concise-encyclopedia-of-chemical-Kirk-Othmer/828891d73aa8a83d1d1ecac5ddfd186cbd35223c

[15] Kumar R, Rana D, Umar A, Sharma P, Chauhan S, Chauhan MS. Ag-doped ZnO nanoellipsoids: potential scaffold for photocatalytic and sensing applications. Talanta. 2015;137:204-213. https://doi.org/10.1016/j.talanta.2015.01.039

[16] Li B, Zhang Z, Wu M. Flow-injection chemiluminescence determination of captopril using on-line electrogenerated silver (II) as the oxidant. Microchemical Journal. 2001;70(2):85-91. /https:/doi.org/10.1016/S0026-265X(01)00090-X

[17] McAdam K, Kimpton H, Essen S, Davis P, Vas C, Wright C, et al. Analysis of hydrazine in smokeless tobacco products by gas chromatography–mass spectrometry. Chemistry Central Journal. 2015;9(1):1-12. https://doi.org/10.1186/s13065-015-0089-0

[18] Song L, Gao D, Li S, Wang Y, Liu H, Jiang Y. Simultaneous quantitation of hydrazine and acetylhydrazine in human plasma by high performance liquid chromatography-tandem mass spectrometry after derivatization with p-tolualdehyde. Journal of Chromatography B. 2017;1063:189-195. https://doi.org/10.1016/j.jchromb.2017.08.036

[19] George M, Nagaraja KS, Balasubramanian N. Spectrophotometric determination of hydrazine. Talanta. 2008;75(1):27-31. https://doi.org/10.1016/j.talanta.2007.09.002

[20] Fan J, Kong J, Feng S, Wang J, Peng P. Kinetic fluorimetric determination of trace hydrazine in environmental waters. International Journal of Environmental and Analytical Chemistry. 2006;86(13):995-1005. https://doi.org/10.1080/03067310600739475

[21] Kumar R, Chauhan MS, Dar GN, Ansari SG, Wilson J, Umar A, et al. ZnO nanoparticles: Efficient material for the detection of hazardous chemical. Sensor Letters. 2014; 12(9):1393-1398. https://doi.org/10.1166/sl.2014.3358

[22] Karthik R, Sasikumar R, Chen SM, Govindasamy M, Kumar JV, Muthuraj V. Green synthesis of platinum nanoparticles using quercus glauca extract and its electrochemical oxidation of hydrazine in water samples. Int. J. Electrochem. Sci. 2016;11:8245-8255.

[23] Faisal M, Harraz FA, Al-Salami AE, Al-Sayari SA, Al-Hajry A, Al-Assiri MS. Polythiophene/ZnO nanocomposite-modified glassy carbon electrode as efficient electrochemical hydrazine sensor. Materials Chemistry and Physics. 2018;214:126-134. https://doi.org/10.1016/j.matchemphys.2018.04.085

[24] Gwiazda M, Bhardwaj SK, Kijeńska-Gawrońska E, Swieszkowski W, Sivasankaran U, Kaushik A. Impedimetric and plasmonic sensing of collagen I using a half-antibody-supported, Au-modified, self-assembled monolayer system. Biosensors. 2021;11(7):227. https://www.mdpi.com/2079-6374/11/7/227

[25] Zhang R, Moon KS, Lin W, Wong CP. Preparation of highly conductive polymer nanocomposites by low temperature sintering

of silver nanoparticles. J. Mater. Chem. 2010;20(10):2018-2023. https://doi.org/10.1039/B921072E

[26] Zhang C, Cui Y, Yang Y, Lu L, Yu S, Meng Z, et al. Highly conductive amorphous pentlandite anchored with ultrafine platinum nanoparticles for efficient pH-universal hydrogen evolution reaction. Advanced Functional Materials. 2021:2105372. https://doi.org/10.1002/adfm.202105372

[27] Watanabe K, Taniguchi T, Kanda H. Direct-bandgap properties and evidence for ultraviolet lasing of hexagonal boron nitride single crystal. Nature Mater. 2004;3(6):404-409. https://doi.org/10.1038/nmat1134

[28] Lin Y, Connell JW. Advances in 2D boron nitride nanostructures: nanosheets, nanoribbons, nanomeshes, and hybrids with graphene. Nanoscale. 2012;4(22):6908-6939. https://doi.org/10.1039/C2NR32201C

[29] Na J, Lee YT, Lim JA, Hwang DK, Kim GT, Choi WK, et al. Few-layer black phosphorus field-effect transistors with reduced current fluctuation. ACS Nano. 2014;8(11):11753-11762. https://doi.org/10.1021/nn5052376

[30] Xue T, Bongu SR, Huang H, Liang W, Wang Y, Zhang F, et al. Ultrasensitive detection of microRNA using a bismuthene-enabled fluorescence quenching biosensor. Chem. Commun. 2020;56(51):7041-7044. https://doi.org/10.1039/D0CC01004A

[31] Gibaja C, Rodriguez-San-Miguel D, Ares P, Gómez-Herrero J, Varela M, Gillen R, et al. Few-layer antimonene by liquid-phase exfoliation. Angewandte Chemie. 2016;128(46):14557-14561. https://doi.org/10.1002/ange.201605298

[32] Sharma PK, Ruotolo A, Khan R, Mishra YK, Kaushik NK, Kim NY, Kaushik AK. Perspectives on 2D-borophene flatland for smart bio-sensing. Materials Letters. 2022;308:131089. https://doi.org/10.1016/j.matlet.2021.131089

[33] Khunger A, Kaur N, Mishra YK, Chaudhary GR, Kaushik A. Perspective and prospects of 2D MXenes for smart biosensing. Materials Letters. 2021;304:130656. https://doi.org/10.1016/j.matlet.2021.130656

[34] Kujawska M, Bhardwaj SK, Mishra YK, Kaushik A. Using graphene-based biosensors to detect dopamine for efficient parkinson's disease diagnostics. Biosensors. 2021;11(11):433. https://doi.org/10.3390/bios11110433

[35] Bhardwaj SK, Mujawar M, Mishra YK, Hickman N, Chavali M, Kaushik A. Bio-inspired graphene-based nano-systems for biomedical applications. Nanotechnology. 2021;32(50):502001. https://iopscience.iop.org/article/10.1088/1361-6528/ac1bdb/meta

[36] Naguib M, Mashtalir O, Carle J, Presser V, Lu J, Hultman L, et al. Two-dimensional transition metal carbides. ACS Nano. 2012;6(2):1322-1331. https://doi.org/10.1021/nn204153h

[37] Rathee G, Bartwal G, Rathee J, Mishra YK, Kaushik A, Solanki PR. Emerging multi-model zirconia nanosystems for high-performance biomedical applications. Advanced NanoBiomed Research. 2021:2100039. https://doi.org/10.1002/anbr.202100039

[38] Singh A, Kaushik A, Dhau JS, Kumar R. Exploring coordination preferences and biological applications of pyridyl-based organochalcogen (Se, Te) ligands. Coordination Chemistry Reviews. 2022;450:214254. https://doi.org/10.1016/j.ccr.2021.214254

[39] Huang H, Feng W, Chen Y. Two-dimensional biomaterials: material science, biological effect and biomedical engineering applications. Chem. Soc. Rev. 2021. https://doi.org/10.1039/D0CS01138J

[40] Sen K, Ali S, Singh D, Singh K, Gupta N. Development of metal free melamine modified graphene oxide for electrochemical sensing of epinephrine. FlatChem. 2021;30:100288. https://doi.org/10.1016/j.flatc.2021.100288

[41] Gusakova J, Wang X, Shiau LL, Krivosheeva A, Shaposhnikov V, Borisenko V, et al. Electronic properties of bulk and monolayer TMDs: theoretical study within DFT framework (GVJ-2e method). Physica Status Solidi (a). 2017;214(12):1700218. https://doi.org/10.1002/pssa.201700218

[42] Lin L, Zhang S, Allwood DA. Transition Metal Dichalcogenides for Energy Storage Applications. In two dimensional transition metal dichalcogenides. Springer, Singapore. 2019:173-201. https://doi.org/10.1007/978-981-13-9045-6_6

[43] Li H, Lu G, Yin Z, He Q, Li H, Zhang Q,et al. Optical identification of single-and few-layer MoS_2 sheets. Small. 2012;8(5):682-686. https://doi.org/10.1002/smll.201101958

[44] Mak KF, Lee C, Hone J, Shan J, Heinz TF. Atomically thin MoS_2: a new direct-gap semiconductor. Physical Review Letters. 2010;105(13):136805. https://doi.org/10.1103/PhysRevLett.105.136805

[45] Wei XL, Zhang H, Guo GC, Li XB, Lau WM, Liu LM. Modulating the atomic and electronic structures through alloying and heterostructure of single-layer MoS_2. J. Mater. Chem. A. 2014;2(7):2101-2109. https://doi.org/10.1039/C3TA13659K

[46] Hui YY, Liu X, Jie W, Chan NY, Hao J, Hsu YT, et al. Exceptional tunability of band energy in a compressively strained trilayer MoS_2 sheet. ACS Nano. 2013;7(8):7126-7131. https://doi.org/10.1021/nn4024834

[47] Liu F, Zhou J, Zhu C, Liu Z. Electric field effect in two-dimensional transition metal dichalcogenides. Advanced Functional Materials. 2017;27(19):1602404. https://doi.org/10.1002/adfm.201602404

[48] Tontini G, Semione GD, Bernardi C, Binder R, de Mello JD, Drago V. Synthesis of nanostructured flower-like MoS_2 and its friction properties as additive in lubricating oils. Industrial Lubrication and Tribology. 2016. http://dx.doi.org/10.1108/ILT-12-2015-0194

[49] Mehta SK, Singh K, Umar A, Chaudhary GR, Singh S. Ultra-high sensitive hydrazine chemical sensor based on low-temperature grown ZnO nanoparticles. Electrochimica Acta. 2012;69:128-133. https://doi.org/10.1016/j.electacta.2012.02.091

[50] Kumar R, Rana D, Umar A, Sharma P, Chauhan S, Chauhan MS. Iron-doped ZnO nanoparticles as potential scaffold for hydrazine chemical sensor. Sensor Letters. 2014;12(8):1273-1278. https://doi.org/10.1166/sl.2014.3354

[51] Mehta SK, Singh K, Umar A, Chaudhary GR and Singh S. Well-crystalline α-Fe_2O_3 nanoparticles for hydrazine chemical sensor application. Science of Advanced Materials. 2011;3(6):962-967. https://doi.org/10.1166/sam.2011.1244

[52] Raoof JB, Ojani R, Jamali F, Hosseini SR. Electrochemical detection of hydrazine using a copper oxide nanoparticle modified glassy carbon electrode. Caspian J. Chem. 2012;1(1):73-85. http://caschemistry.journals.umz.ac.ir/article_291_8949986e9d8ef024dbdcbc69096dc867.pdf

[53] Feng F, Ma Z. Sensitive electrochemical detection of hydrazine based on hollow core-satellite hZnS@ Au nanoparticles. Sensors and Actuators B: Chemical. 2016;232:9-15. https://doi.org/10.1016/j.snb.2016.03.127

[54] Lee JY, Nguyen TL, Park JH, Kim BK. Electrochemical detection of hydrazine using poly (dopamine)-modified electrodes. Sensors.

2016;16(5):647. https://doi.org/10.3390/s16050647

[55] Siangproh W, Chailapakul O, Laocharoensuk R, Wang J. Microchip capillary electrophoresis/electrochemical detection of hydrazine compounds at a cobalt phthalocyanine modified electrochemical detector. Talanta. 2005;67(5):903-907. https://doi.org/10.1016/j.talanta.2005.04.024

[56] Zhang J, Gao W, Dou M, Wang F, Liu J, Li Z, Ji J. Nanorod-constructed porous Co_3O_4 nanowires: highly sensitive sensors for the detection of hydrazine. Analyst. 2015;140(5):1686-1692. /doi.org/10.1039/C4AN02111H

[57] Yi Q, Niu F, Yu W. Pd-modified TiO_2 electrode for electrochemical oxidation of hydrazine, formaldehyde and glucose. Thin Solid Films. 2011;519(10):3155-3161. https://doi.org/10.1016/j.tsf.2010.12.241